Available online at www.sciencedirect.com
ScienceDirect
Toxicology and Applied Pharmacology 217 (2006) 252–259
Toxicology and Applied Pharmacology
www.elsevier.com/locate/ytaap

In vitro toxicity of silica nanoparticles in human lung cancer cells

Weisheng Lin [a], Yue-wern Huang [b], Xiao-Dong Zhou [c], Yinfa Ma [a,*]

[a] Department of Chemistry and Environmental Research Center, University of Missouri–Rolla, Rolla, MO 65409, USA
[b] Department of Biological Sciences and Environmental Research Center, University of Missouri–Rolla, Rolla, MO 65409, USA
[c] Pacific Northwest National Laboratory, Richland, WA 99352, USA

Received 28 July 2006; revised 2 October 2006; accepted 2 October 2006
Available online 6 October 2006

Abstract

The cytotoxicity of 15-nm and 46-nm silica nanoparticles was investigated by using crystalline silica (Min-U-Sil 5) as a positive control in cultured human bronchoalveolar carcinoma-derived cells. Exposure to 15-nm or 46-nm SiO_2 nanoparticles for 48 h at dosage levels between 10 and 100 μg/ml decreased cell viability in a dose-dependent manner. Both SiO_2 nanoparticles were more cytotoxic than Min-U-Sil 5; however, the cytotoxicities of 15-nm and 46-nm silica nanoparticles were not significantly different. The 15-nm SiO_2 nanoparticles were used to determine time-dependent cytotoxicity and oxidative stress responses. Cell viability decreased significantly as a function of both nanoparticle dosage (10–100 μg/ml) and exposure time (24 h, 48 h, and 72 h). Indicators of oxidative stress and cytotoxicity, including total reactive oxygen species (ROS), glutathione, malondialdehyde, and lactate dehydrogenase, were quantitatively assessed. Exposure to SiO_2 nanoparticles increased ROS levels and reduced glutathione levels. The increased production of malondialdehyde and lactate dehydrogenase release from the cells indicated lipid peroxidation and membrane damage. In summary, exposure to SiO_2 nanoparticles results in a dose-dependent cytotoxicity in cultural human bronchoalveolar carcinoma-derived cells that is closely correlated to increased oxidative stress.

Keywords: Silica (SiO_2); Cytotoxicity; Lung cancer cells (A549); Nanoparticles; Oxidative stress

Introduction

Nanomaterials are defined by the U.S. National Nanotechnology Initiative as materials that have at least one dimension in the 1- to 100-nm range. Due to their unique physical and chemical characteristics, nanotechnology has become one of the leading technologies over the past 10 years (Stix, 2001). There is enormous interest in applying nanomaterials in a variety of industries. As a non-metal oxide, silica (SiO_2) nanoparticles have found extensive applications in chemical mechanical polishing and as additives to drugs, cosmetics, printer toners, varnishes, and food. In recent years, the use of SiO_2 nanoparticles has been extended to biomedical and biotechnological fields, such as biosensors for simultaneous assay of glucose, lactate, L-glutamate, and hypoxanthine levels in rat striatum (Zhang et al., 2004), biomarkers for leukemia cell identification using optical microscopy imaging (Santra et al., 2001), cancer therapy (Hirsch et al., 2003), DNA delivery (Bharali et al., 2005; Gemeinhart et al., 2005), drug delivery (Venkatesan et al., 2005), and enzyme immobilization (Qhobosheane et al., 2001).

Thus, the environmental and health impact of nanomaterials is of great interest. The cytotoxicity associated nanoparticle exposure is to some degree particle specific. Exposure to silica at micro-scale size is associated with the development of several autoimmune diseases, including systemic sclerosis, rheumatoid arthritis, lupus, and chronic renal disease, while certain crystalline silica polymorphs may cause silicosis and lung cancer (IARC, 1997; Donaldson and Borm, 1998; Shi et al., 1998; Fubini and Hubbard, 2003; Rimal et al., 2005). Size-dependent effects of particles have been well documented. For instance, differential toxicity between micro- and nanoscale materials has been observed in TiO_2 particles (Oberdörster, 2000), polystyrene particles (Brown et al., 2001), and mineral fibers (Donaldson and Tran, 2002). Thus, it is likely that the unique properties (i.e., small size and corresponding large specific surface area) of

* Corresponding author. Fax: +1 573 341 6033.
E-mail address: yinfa@umr.edu (Y. Ma).

0041-008X/$ - see front matter © 2006 Elsevier Inc. All rights reserved.
doi:10.1016/j.taap.2006.10.004

nano-sized SiO_2 may impose biological effects that are quite different from its micro-scale particles.

Studies have demonstrated that SiO_2 nanoparticles cause aberrant clusters of topoisomerase I (topo I) in the nucleoplasm in cells, pro-inflammatory stimulation of endothelial cells, and fibrogenesis in Wistar rats (Chen et al., 2004; Peters et al., 2004; Chen and von Mikecz, 2005). On the other hand, an *in vivo* mouse study showed that silica nanoparticles are not toxic and, therefore, can be used *in vivo* (Xue et al., 2006). Thus, the effects and mechanisms of toxicity in nanoscale size SiO_2 particles on human health warrant further studies.

The first objective of this study was to evaluate cytotoxicity of SiO_2 nanoparticles (15 nm, 46 nm) in human bronchoalveolar carcinoma-derived cells (A549). Crystalline silica (Min-U-Sil 5), a well-documented occupational health hazard, was used as a positive control (IARC, 1997; Donaldson and Borm, 1998; Shi et al., 1998; Fubini and Hubbard, 2003; Rimal et al., 2005). The second object was to study the oxidative stress mechanism induced by 15-nm SiO_2 nanoparticles. In the present study, particles were dispersed in the cell culture medium at varying concentrations and then dosed to cells. Cytotoxicity was measured by determining cell viability using the sulforhodamine B (SRB) method (Skehan et al., 1990). To elucidate the possible mechanisms of cytotoxicity, biomarkers for cytotoxicity and oxidative stress, namely reactive oxygen species (ROS), glutathione (GSH), malondialdehyde (MDA), and lactate dehydrogenase (LDH), were measured using 2′,7′-dichlorofluorescin diacetate (DCFH-DA), high performance liquid chromatography (HPLC), and LDH assay.

Materials and methods

Nanoparticles. In our previous study, 15-nm SiO_2 nanoparticles showed significant cytotoxicity at 10–100 μg/ml range (unpublished data). To study the size effect of SiO_2 nanoparticles and the oxidative stress mechanism, 15-nm and 46-nm SiO_2 nanoparticles were selected for this study. The SiO_2 nanoparticles (15 nm, 46 nm) used in this study were supplied by Degussa Co. (Parsippany, NJ, USA). Crystalline silica (Min-U-Sil 5) was obtained from U.S. Silica Company (Berkeley Springs, WV, USA). According to the company's data sheet, more than 98% of the crystalline silica particles were less than 5 μm in diameter and quartz purity was 99.4%.

The particle sizes and distribution of SiO_2 nanoparticles were measured by Philips EM430 transmission electron microscopy (TEM) (Philips Electron Optics, Eindhoven, Holland). Crystal structure was characterized by Scintag XDS 2000 diffractometer (Scintag, Inc., Cupertino, CA, USA). The surface area of the particles was determined by Quantachrome Autosorb 1-C (Boynton, FL, USA). The characterization results are shown in Table 1.

The major trace metal impurities in 15-nm and 46-nm SiO_2 nanoparticles were measured using a Perkin-Elmer ELAN DRC-e Inductively Coupled Plasma–Mass Spectrometry (ICP-MS) system (Perkin-Elmer, Wellesley, MA, USA). The ICP-MS conditions were set up as follows: vacuum pressure: 6.5×10^{-6} Torr; nebulizer gas flow: 0.98 l/min; ICP RF power: 1200 W; lens voltage: 7.6 V; analog stage voltage: −1700 V; pulse stage voltage: 1100 V. The data are presented in Table 2. The metal impurity data of Min-U-Sil 5 were provided by U.S. Silica Company.

Table 1
Characterization of 15 nm SiO_2, 46 nm SiO_2 and Min-U-Sil 5

	Size and distribution nm (mean±std)	Surface area (m^2/g)	Crystalline structure
15 nm SiO_2	15±5	268.01	Amorphous
46 nm SiO_2	46±12	52.48	Amorphous
Min-U-Sil 5	629±272	6.35	Crystal

The size, surface area, and crystalline structure were determined by TEM, BET surface area analyzer, and X-ray diffraction (XRD), respectively.

Table 2
Metal impurity levels in SiO_2 nanoparticles and Min-U-Sil 5

Elements	SiO_2 nanoparticles (15 nm and 46 nm)[a] (ppb)	Crystalline Silica (Min-U-Sil 5)[b] (%)
Na	<40	<0.01
Mg	<40	0.01
Al	<40	0.14
K	<40	0.02
Ca	~40	0.01
Ti	<40	0.01
Fe	<40	0.02

[a] Our ICP-MS analysis data.
[b] Provided by U. S. Silica Company. Twenty-eight elements tested in our ICP-MS system and all of their levels were below the detection limits (40 ppb), except that of Ca. Seven elements listed are compared with the data provided by U.S. Silica Company. Elements not tabulated included Be, V, Cr, Mn, Co, Ni, Cu, Zn, As, Se, Rb, Sr, Mo, Ag, Cd, Sb, Cs, Ba, Bi, Pb, U.

Due to their nanoscale size and surface properties, nanoparticles tend to aggregate or precipitate in suspensions. Average hydrodynamic size and standard deviation of SiO_2 nanoparticles were determined by dynamic light scattering using a Nanotrac NPA250 (Microtrac, North Largo, FL, USA). Particle size was analyzed by suspending particles in Millipore water.

Suspensions of SiO_2 nanoparticles and Min-U-Sil 5 were prepared in the cell culture medium and dispersed by a sonicator (FS-60H, 130W, 20kHz, Fisher Scientific, Pittsburgh, PA, USA). In each study, the suspension was freshly prepared and diluted to three concentrations (10 μg/ml, 50 μg/ml, and 100 μg/ml) and then immediately applied to the A549 cells.

Chemicals. Fetal bovine serum was purchased from American Type Culture Collection (ATCC) (Manassas, VA, USA). Ham's F-12 medium with L-glutamine, HPLC grade n-butanol, acetonitrile, and analytical grade 12 M hydrochloric acid were purchased from Fisher Scientific (Pittsburgh, PA, USA). Trypsin–EDTA (1×) and Hank's balanced salt solution (HBSS) were purchased from Invitrogen Co. (Carlsbad, CA, USA). Sulforhodamine B was bought from ICN Biomedicals (Irvine, CA, USA). Penicillin-streptomycin, trichloroacetic acid (TCA), 1,1,3,3-tetramethoxypropane, 2-thiobarbituric acid, 2-vinylpyridine, *o*-phosphoric acid (HPLC grade), *N*-(1-pyrenyl)maleimide (NPM), 2′,7′-dichlorofluorescin diacetate, glutathione (reduced), L-serine, boric acid, diethylenetriaminepentaacetic acid (DETAPAC), TRIS hydrochloride, butylatedhydroxytoluene (BHT), tetrahydrofuran, Na_2HPO_4, NaH_2PO_4, and acetic acid (HPLC grade) were obtained from Sigma-Aldrich (Saint Louis, MO, USA). Ultrapure DI-water was prepared using a Milli-Q system (Millipore, Bedford, MA, USA).

Cell culture and treatment with SiO_2. The human bronchoalveolar carcinoma-derived cell line, A549, was purchased from ATCC (Manassas, VA, USA). This cell line has been widely used in *in vitro* cytotoxicity studies (Huang et al., 2004; Bakand et al., 2006). Cells were maintained in Ham's F-12 medium supplemented with 10% fetal bovine serum, 100 U/ml penicillin, and 100 μg/ml streptomycin, and grown at 37 °C in a 5% CO_2 humidified environment. For the SRB assay, A549 cells were plated into a 24-well plate at a density of 1.0×10^4 cells per well in 1.0 ml culture medium and allowed to attach for 48 h. For the determination of GSH, MDA, and LDH levels, A549 cells were plated into 75-cm^2 flasks at a density of 2.0×10^5 cells per flask in 13 ml culture medium and allowed to attach for 48 h. Then, the freshly dispersed particles suspensions in cell culture medium were prepared and diluted to appropriate concentrations (10, 50 and 100 μg/ml) and immediately applied to the cells. Cells not exposed to particles served as controls in each experiment. The selection of the 10–100 μg/ml dosage range of SiO_2 nanoparticles was based on a preliminary dose-response study (data not shown). A dosage level lower than 10 μg/ml did not produce cytotoxicity in

A549 cells, while a dosage level higher than 100 μg/ml resulted in severe precipitation in cell media after 48 h. The 48-h exposure time was chosen for investigation on the oxidative stress because of the detection limitations of the assay technique and the required time for particles to produce significant effects. The response (i.e., cell viability) at 24-h exposure was not as pronounced as that at 48 h. In addition, the current technique to measure ROS for longer exposure time possibly limits the accuracy of ROS determination due to the high activity of ROS.

After incubation with SiO_2 nanoparticles for 48 h, the cell culture medium was collected for LDH determination. The cells were rinsed with ice-cold PBS and trypsinized. Homogenates were frozen at −70 °C until analyzed for levels of GSH, MDA, and protein. For ROS determination, cells were plated at a density of 1.0×10^5 cells/well in a 24-well collagen-coated culture plate and allowed to attach for 48 h; the total ROS was then measured as described below.

Assessment of cytotoxicity. After the exposure of cells to SiO_2 nanoparticles or Min-U-Sil 5 for 24, 48, and 72 h, the medium was removed and the number of cells in each well was determined using the sulforhodamine B (SRB) assay. Briefly, cells were fixed with 500 μl of cold 10% trichloroacetic acid (TCA) for 1 h. The TCA solution was then discarded, and the cells were washed three times with distillated water followed by drying under nitrogen. Five hundred microliters of 0.2% sulforhodamine B in a 1% acetic acid was added to each well to stain the cells for 30 min. The staining solution was discarded, and the cells were washed with 1% acetic acid to eliminate excess dye. After complete drying, the dye in each well was dissolved in 300 μl of cold 10 mM Tris buffer (pH 10.5). One hundred microliters of dye solution was transferred into a 96-well plate and absorbance was measured at 550 nm using a microplate reader (FLOURstar, BMG Labtechnologies, Durham, NC, USA).

LDH measurement. Lactate dehydrogenase (LDH) activity in the cell medium was determined using a commercial LDH Kit (Pointe Scientific, Inc., Lincoln Park, MI, USA). One hundred microliters of cell medium was used for LDH analysis. Absorption was measured using a Beckman DU-640B UV–Visible Spectrophotometer at 340 nm. This procedure is based on the method developed by Wacker et al. (1956), optimized for greater sensitivity and linearity. Released LDH catalyzed the oxidation of lactate to pyruvate with simultaneous reduction of NAD^+ to NADH. The rate of NAD^+ reduction was measured as an increase in absorbance at 340 nm. The rate of NAD^+ reduction was directly proportional to LDH activity in the cell medium.

Intracellular ROS measurement. The production of intracellular reactive oxygen species (ROS) was measured using 2′,7′-dichlorofluorescin diacetate (DCFH-DA) (Wang and Joseph, 1999). DCFH-DA passively enters the cell where it reacts with ROS to form the highly fluorescent compound dichlorofluorescein (DCF). Briefly, 10 mM DCFH-DA stock solution (in methanol) was diluted 500-fold in HBSS without serum or other additive to yield a 20 μM working solution. After 48 h of exposure to SiO_2 nanoparticles, the cells in the 24-well plate were washed twice with HBSS and then incubated in 2 ml working solution of DCFH-DA at 37 °C for 30 min. Fluorescence was then determined at 485-nm excitation and 520-nm emission using a microplate reader.

GSH measurement. The method developed by Winters et al. was used to determine the cellular GSH levels (Winters et al., 1995). After freezing at −70 °C, the cells were homogenized in serine borate buffer (100 mM Tris–HCl, 10 mM boric acid, 5 mM L-serine, 1 mM DETAPAC, pH 7.5). Twenty microliters homogenate was added to 230 μl HPLC grade H_2O and 750 μl NMP solution (1 mM in acetonitrile). The resulting suspensions were incubated for 5 min at room temperature, and then 5 μl of 2N HCl was added to stop the reaction. The samples were filtered through a 0.2 μm Whatman Puradisc syringe filter (Whatman International Ltd., Maidstone, Kent, UK), and an aliquot of 20 μl was injected for analysis using a PerkinElmer HPLC system (PerkinElmer Inc., Wellesley, MA, USA) with fluorescence detection (excitation at 330 nm, emission at 375 nm) and a 5-μm Reliasil C18 column (250 × 4.6 mm) (Column Engineering, Ontario, CA, USA). The mobile phase consisted of 70% acetonitrile, 30% HPLC H_2O containing 1ml/l acetic acid, and 1 ml/l *o*-phosphoric acid. The flow rate was 1.0 ml/min.

MDA measurement. The cellular concentration of malondialdehyde (MDA) was determined by the method described by Draper et al. with some modifications (Draper et al., 1993). An aliquot of 350 μl of cell homogenate was mixed with 100 μl of 500 ppm BHT in methanol and 550 μl of 10% TCA. The resulting mixture was boiled for 30 min to precipitate the proteins. After cooling on ice, the sample was centrifuged at 1500×*g* for 10 min. The supernatant was collected, and 500 μl was mixed with 500 μl of a saturated aqueous TBA solution. This mixture was heated in a boiling water bath for 30 min. After cooling to room temperature, 500 μl samples were extracted with 1 ml of n-butanol using a Vortex mixer, and then centrifuged at 1000×*g* for 5 min. The top layer was collected and filtered through a 0.2 μm Whatman Puradisc syringe filter, followed by analysis with the same PerkinElmer HPLC system and column that was used for GSH analysis. Excitation and emission wavelengths were set at 515 nm and 550 nm, respectively. Twenty microliters samples were injected for analysis. The mobile phase consisted of 69.4% 5 mM sodium phosphate buffer (pH 7.0), 30% acetonitrile, and 0.6% THF. The flow rate of the mobile phase was 1.0 ml/min.

Protein assay. The total protein concentration was measured by the Bradford method (Bradford, 1976) using a BioRad Assay Kit (BioRad, Richmond, CA, USA) and bovine serum albumin as the standard.

Statistics. Data were expressed as the mean±SD from three independent experiments. One-tailed unpaired Student's *t*-test was used for significance testing, using a p value of 0.05.

Results

Particle characterization

The results from characterization of 15-nm SiO_2, 46-nm SiO_2 and Min-U-Sil 5 were summarized in Table 1. The mean size and distribution of these three types of particles were 15± 5 nm, 46±12 nm, and 629±272 nm, respectively. The surface areas by BET measurement were 268.01, 52.48, and 6.35 m^2/g, respectively. The structure of 15-nm SiO_2 and 46-nm SiO_2 was amorphous while the XRD analysis clearly showed the crystal characteristic of Min-U-Sil 5.

Hydrodynamic size of SiO_2 nanoparticles in suspension

The size measured by a dynamic light scattering method was the particles' hydrodynamic size, which indicates the extent of aggregation of particles in suspension. The hydrodynamic sizes of the 15-nm and 46-nm SiO_2 nanoparticles in water suspension were 590±104 nm and 617±107 nm, respectively, indicating that aggregation occurred and the aggregation was not uniform (relative standard deviation 17.6% and 17.3% respectively).

The dose-dependent cytotoxicity of SiO_2 nanoparticles and Min-U-Sil 5

After A549 cells were exposed to SiO_2 nanoparticles (15 nm, 46 nm) or Min-U-Sil 5 at 10, 50, and 100 μg/ml for 48 h, cell viability decreased as a function of dosage levels (Fig. 1). Cell viability of the groups exposed to 15-nm SiO_2 nanoparticles decreased to 91.9%, 76.0%, and 68.1%, respectively, compared to the control group ($ps < 0.05$). Interestingly,

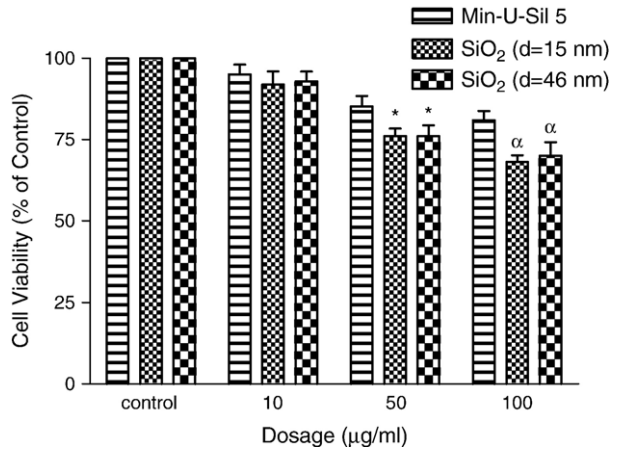

Fig. 1. Viability of A549 cells after 48-h exposure to 10 μg/ml, 50 μg/ml, or 100 μg/ml of SiO_2 nanoparticles (15 nm, 46 nm) and Min-U-Sil 5. Values are mean±SD from three independent experiments. Triplicates of each treatment group were used in each independent experiment. Significance indicated by: *$p<0.05$ versus cells exposed to 50 μg/ml Min-U-Sil 5. $^{\alpha}p<0.05$ versus cells exposed to 100 μg/ml Min-U-Sil 5. Min-U-Sil 5 was used as the positive control in this study, and the cell viability of the groups exposed to Min-U-Sil 5 (10, 50, 100 μg/ml) decreased significantly to 95.1%, 85.2%, and 81.0%, respectively, compared to the control group ($ps<0.05$).

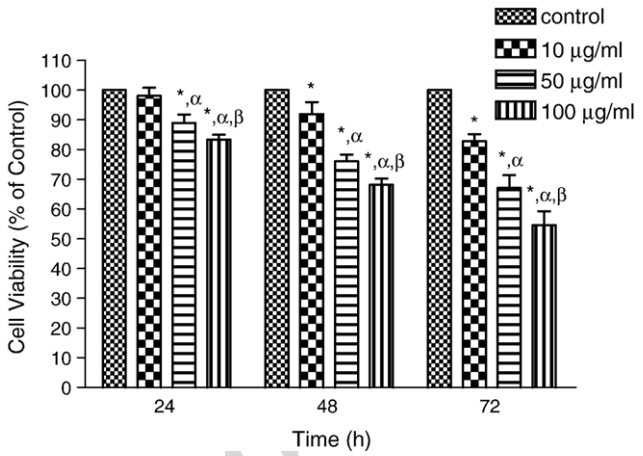

Fig. 2. Viability of A549 cells after 24-h, 48-h, and 72-h exposure to 10 μg/ml, 50 μg/ml, or 100 μg/ml of 15 nm SiO_2 nanoparticles. Values are mean±SD from three independent experiments. Triplicates of each treatment group were used in each independent experiment. Significance indicated by: *$p<0.05$ versus control cells; $^{\alpha}p<0.05$ versus cells exposed to 10 μg/ml SiO_2; $^{\beta}p<0.05$ versus cells exposed to 50 μg/ml SiO_2.

the cytotoxicity of the 46-nm SiO_2 nanoparticles, which caused decreases of cell viability of 92.9%, 76.0%, and 70.1%, respectively, was not significantly different from that of the 15-nm SiO_2 nanoparticles. Both the 15-nm and 46-nm nanoparticles showed significantly higher cytotoxicity at 50 and 100 μg/ml dosages than the Min-U-Sil 5, a positive control. Due to the similarity of cytotoxicity associated with these two sizes of nanoparticles, only 15-nm SiO_2 nanoparticles were used in subsequent time course as well as the mechanism studies.

Time course and dose-dependent cytotoxicity of 15-nm SiO_2 nanoparticles

A549 cells were exposed to SiO_2 at 10, 50, and 100 μg/ml dosage levels for 24 h, 48 h, and 72 h. Cell viability decreased as a function of both concentration and time (Fig. 2). The dose-dependent cell viabilities at 24 h were 98.0%, 88.9%, and 83.4%, followed by a reduction to 91.9%, 76.0%, and 68.1% at 48 h exposure. After 72-h exposure, cell numbers had decreased to 82.8%, 67.1%, and 54.6%, compared to the control.

Cellular oxidative stress level and lipid peroxidation induced by exposure to 15-nm SiO_2 nanoparticles

DCF fluorescence intensity, indicative of oxidative stress (OS) in the cells, increased after 48-h exposure to 15-nm SiO_2 nanoparticles at all concentrations examined. Compared to the controls, DCF fluorescence intensity increased by 70%, 139%, and 181% after exposure to 10, 50, and 100 μg/ml of 15-nm SiO_2 nanoparticles, respectively (Fig. 3, $ps<0.05$). Cellular GSH level exhibited a dose-dependent decrease (Fig. 4). The GSH levels were reduced by 8.3%, 12.5%, and 22.4% after 48-h exposure to 15-nm SiO_2 nanoparticles at the three exposure levels ($ps<0.05$). There was a significant correlation between ROS levels and GSH levels ($R^2=0.980$) (Fig. 5).

Cellular levels of MDA were significantly increased after exposure to SiO_2 nanoparticles for 48 h (Fig. 6). The MDA levels were elevated by 10.9%, 12.8%, and 17.0% at the three respective exposure levels compared to the control groups ($ps<0.05$).

Release of LDH resulted from exposure to 15-nm SiO_2 nanoparticles

The cell membrane damage was reflected in the elevated LDH levels in the cell medium after cells were exposed to 15-nm SiO_2 nanoparticles for 48 h (Fig. 7; $ps<0.05$). The LDH levels were increased by 8.7%, 12.5%, and 17.7% following

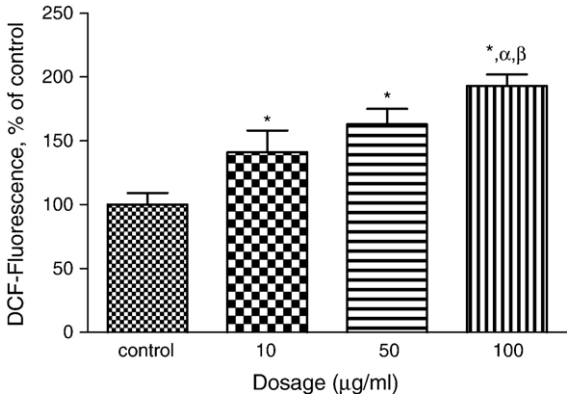

Fig. 3. DCF-fluorescence intensity after 48-h exposure to 10 μg/ml, 50 μg/ml, or 100 μg/ml of 15 nm SiO_2 nanoparticles. Values are mean±SD from three independent experiments. Triplicates of each treatment group were used in each independent experiment. Significance indicated by: *$p<0.05$ versus control cells; $^{\alpha}p<0.05$ versus cells exposed to 10 μg/ml SiO_2; $^{\beta}p<0.05$ versus cells exposed to 50 μg/ml SiO_2.

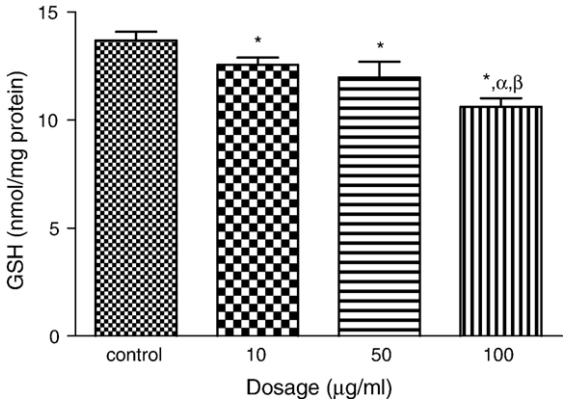

Fig. 4. Cellular GSH levels of A-549 cells after 48-h exposure to 10 μg/ml, 50 μg/ml, or 100 μg/ml of 15 nm SiO_2. Values are mean±SD from three independent experiments. Significance indicated by: *$p<0.05$ versus control cells; $^{\alpha}p < 0.05$ versus cells exposed to 10 μg/ml SiO_2; $^{\beta}p<0.05$ versus cells exposed to 50 μg/ml SiO_2.

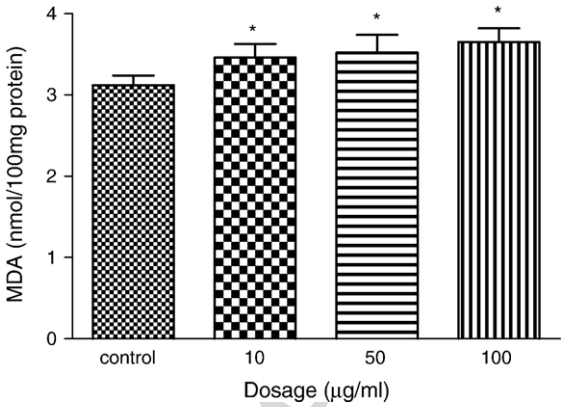

Fig. 6. Cellular MDA levels of A-549 cells after 48-h exposure to 10 μg/ml, 50 μg/ml, or 100 μg/ml of 15 nm SiO_2 nanoparticles. Values are mean±SD from three independent experiments. Significance indicated by: *$p<0.05$ versus control cells.

exposure to 10 μg/ml, 50 μg/ml, and 100 μg/ml of SiO_2 nanoparticles, respectively. A linear correlation was observed between LDH activity and cell viability ($R^2=0.924$). Cell viability was also highly correlated with the levels of ROS ($R^2=0.942$) (Fig. 8).

Discussion

To date, there are very few studies investigating the toxic effects of nanomaterials, and no guidelines are presently available to quantify these effects. In this study, the cytotoxicity of two sizes of SiO_2 nanoparticles (15 nm, 46 nm) was investigated in cultured human bronchoalveolar carcinoma-derived cells along with crystalline silica (Min-U-Sil 5) as a positive control. The cytotoxicity of the 15-nm and 46-nm SiO_2 nanoparticles were not significantly different from each other in the 10–100 μg/ml dosage range. As expected, exposure to crystalline silica results in significant reduced cell viability (as shown in Fig. 1). Interestingly, both sizes of SiO_2 nanoparticles produced greater cytotoxicity than the crystalline silica in the 50–100 μg/ml dosage range. In an *in vivo* study, Warheit et al. (2005) also found that 10 nm SiO_2 nanoparticles produced a greater pulmonary inflammatory response than Min-U-Sil quartz particles (average diameter of 1.6 μm) after instillation of particles into the lungs of rats at doses of 1 or 5 mg/kg. However, in a separate experiment of the same study, authors found an opposite order of inflammatory potency as 50-nm SiO_2 nanoparticles versus Min-U-Sil quartz particles. Therefore, more experiments and mechanism studies are required to elucidate the cytotoxic difference between nanoscale SiO_2 and micro-scale SiO_2. Regarding the complexity and diverse properties of particles, such as composition, size, shape, surface activities, surface treatment, and crystallinity, a study only based on size may be misleading if other variables are involved. Complete evaluation of the effects of various particle properties is necessary (Oberdorster et al., 2005). In this study, crystalline silica (Min-U-Sil 5) served as a positive control material for cytotoxicity evaluation of two SiO_2 nanoparticles (15 nm, 46 nm), not for micro-scale versus nanoscale comparison because their crystal structures are different.

Our study showed that 15-nm and 46-nm SiO_2 exhibited similar cytotoxicity. Thus, 15-nm SiO_2 nanoparticles were used to study nanoparticle-induced oxidative stress in A549 cells.

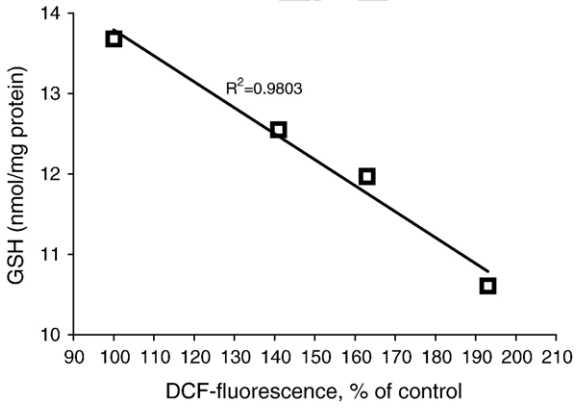

Fig. 5. Correlation between ROS and GSH levels after 48-h exposure to 10 μg/ml, 50 μg/ml, or 100 μg/ml of 15-nm SiO_2 nanoparticles.

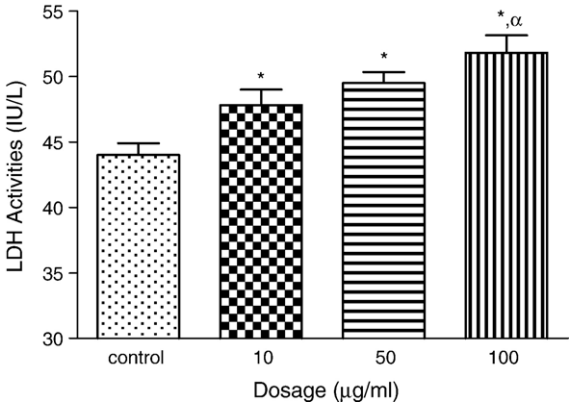

Fig. 7. The LDH activities in the cell culture medium after 48-h exposure to 10 μg/ml, 50 μg/ml, or 100 μg/ml of 15-nm SiO_2 nanoparticles. Values are mean±SD from three independent experiments. Significance indicated by: *$p<0.05$ versus control cells; $^{\alpha}p<0.05$ versus cells exposed to 10 μg/ml SiO_2.

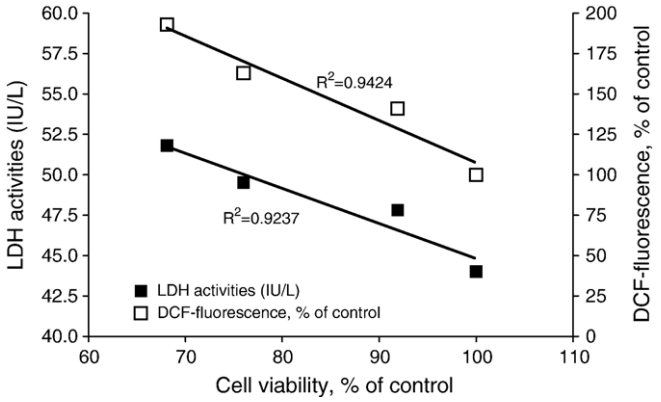

Fig. 8. Correlation between cell viabilities versus LDH and DCF intensity after 48-h exposure to 10 μg/ml, 50 μg/ml, or 100 μg/ml of 15-nm SiO_2 nanoparticles.

The results indicated that 15-nm SiO_2 nanoparticles at dosage levels of 10–100 μg/ml cause both dose- and time-dependent cytotoxicity. Concomitant cellular oxidative stress was manifested by elevated ROS levels, reduced GSH levels, and increased lipid peroxidation. The inverse linear relationship between the ROS level and the GSH level indicated that free radical species were generated by exposure to SiO_2 reduced cellular antioxidant levels ($R^2=0.980$). Moreover, free radicals also resulted in the production of malondialdehyde, indicative of lipid peroxidation. There was a strong correlation between decreased cell viability and increased ROS level after 48-h exposure ($R^2=0.942$). The reverse correlation between the decreased cell viability and the increased LDH activity suggests that cell death is the primary cause of the reduction in cell number. Together, these results indicate that the reduction of cell viability is due to increased cellular stress that leads to increased cell mortality as indicated by released LDH. While both sulforhodamine B (SRB) assay and LDH assay measure cell viability, the LDH provides additional information about cell membrane damage.

Size-dependent cytotoxicity has been well documented. It is generally perceived that the smaller a particle, the greater its toxicity (Kipen and Laskin, 2005; Oberdorster et al., 2005; Nel et al., 2006). Because of the larger specific surface area, the 15-nm SiO_2 particles would be expected to induce higher oxidative stress than the 46-nm SiO_2 particles if all other factors are the same. However, our data showed similar cytotoxicity between 15-nm and 46-nm SiO_2 nanoparticles in the 10–100 μg/ml dosage range. This result may reflect aggregation of SiO_2 nanoparticles in the cultured medium. Based upon our dynamic light scattering data, the 15-nm and 46-nm SiO_2 nanoparticles aggregated to form hydrodynamic sizes of 590 nm and 617 nm, respectively. The similar hydrodynamic sizes of these two nanoparticles might explain the similar cytotoxicities. It is noted that the hydrodynamic sizes were measured in the deionized water instead of in cell medium. The reason is that dynamic light scattering is a function of the relative refractive indices of the particle or molecule and the dispersant. When measurement is carried out in cell medium, the molecules in cell medium will scatter light and cause interference. Consequently, the data cannot be accurately obtained. Several techniques are available to prevent aggregation, including addition of surfactants or modification of particle surface (Bagwe et al., 2006). However, surface modification may affect SiO_2 nanoparticle toxicity by decreasing ROS generation (Fubini and Hubbard, 2003). Sayes et al. (2006) showed altered toxic effects in the presence of surfactants or as a result of surface modification to single-walled carbon nanotubes (SWNT). Their results indicated that as the degree of sidewall modification increases, SWNT become less cytotoxic. In addition, sidewall modified SWNT samples were substantially less cytotoxic than surfactant stabilized SWNTs. In order to prevent alteration in the toxicity of SiO_2 nanoparticles, we freshly dispersed SiO_2 nanoparticles in culture medium immediately before each experiment with no surfactant included in the system.

The detailed mechanism by which ROS are generated is still unclear. However, there is evidence that crystalline silica can induce ROS, such as hydroxyl free radical, at the particle surface (Dalal et al., 1990; Lenz et al., 1992; Carter and Driscoll, 2001; Porter et al., 2006). Enhanced production of $HO^{\cdot}$ by adding H_2O_2 to trace iron(III)-containing crystalline silica suggests that a Fenton reaction occurred on the surface of silica particle (Fubini and Hubbard, 2003). The authors suspected that the relatively high metal impurities in crystalline silica may play a key role to yield $HO^{\cdot}$ radicals via the Fenton reaction ($Fe^{2+}+H_2O_2 \rightarrow Fe^{3+}+OH^{-}+HO^{\cdot}$). However, our ICP-MS data (Table 2) indicate that SiO_2 nanoparticles contain ultra low levels of metal impurities. Thus, our results suggest that SiO_2 nanoparticles generate $HO\cdot$ in the absence of trace metal. Fenoglio et al. also demonstrated that pure quartz and iron-deprived quartz dusts can generate $HO\cdot$ in the absence of trace iron (Fenoglio et al., 2001). The mechanism by which SiO_2 nanoparticles generates ROS warrants further investigation.

In addition to inducing oxidative stress, reduced cell viability by SiO_2 nanoparticles may result from penetration of particles into the cell nucleus. Aberrant clusters of topoisomerase I and protein aggregation may ensue, resulting in functional alterations, such as inhibition of replication, transcription, and cell proliferation (Chen and von Mikecz, 2005). Furthermore, expression of a wide variety of genes has been shown to be sensitive to ROS at the transcriptional level. Among the genes known to be activated by oxidative stress are those for MAP kinase signaling, DNA damage, cAMP/Ca^{2+} signaling, NFkB signaling, PI3-AKT signaling, and apoptosis (Foncea et al., 2000; Kharasch et al., 2006). We are currently studying the expression of genes in these signaling pathways in response to exposure to SiO_2 nanoparticles.

In conclusion, we have demonstrated that 15-nm and 46-nm SiO_2 nanoparticles significantly reduce cell viability in a dose-dependent and time-dependant manner in bronchoalveolar carcinoma-derived cells at 10–100 μg/ml dosage. Both of SiO_2 nanoparticles showed higher cytotoxicity than the positive control material (Min-U-Sil 5). The ROS generated by exposure to 15-nm SiO_2 nanoparticles produce oxidative stress in these cells as reflected by reduced GSH levels and the elevated production of MDA and LDH, indicative of lipid peroxidation and membrane damage.

Acknowledgments

The authors thank the financial support from the Departments of Chemistry and Biological Sciences and the Environmental Research Center at the University of Missouri–Rolla. The authors thank Honglan Shi for providing ICP-MS analysis. The authors also thank Nuran Ercal and Wei Wu for helpful discussions and comments regarding the GSH and MDA protocols. We thank Robert S. Aronstam for commenting and editing the manuscript.

Appendix A. Supplementary data

Supplementary data associated with this article can be found, in the online version, at doi:10.1016/j.taap.2006.10.004.

References

Bagwe, R.P., Hilliard, L.R., Tan, W., 2006. Surface modification of silica nanoparticles to reduce aggregation and nonspecific binding. Langmuir 22, 4357–4362.

Bakand, S., Winder, C., Khalil, C., Hayes, A., 2006. A novel in vitro exposure technique for toxicity testing of selected volatile organic compounds. J. Environ. Monit. 8, 100–105.

Bharali, D.J., Klejbor, I., Stachowiak, E.K., Dutta, P., Roy, I., Kaur, N., Bergey, E.J., Prasad, P.N., Stachowiak, M.K., 2005. Organically modified silica nanoparticles: a nonviral vector for in vivo gene delivery and expression in the brain. Proc. Natl. Acad. Sci. U. S. A. 102, 11539–11544.

Bradford, M.M., 1976. A rapid and sensitive method for the quantitation of microgram quantities of protein utilizing the principle of protein-dye binding. Anal. Biochem. 72, 248–254.

Brown, D.M., Wilson, M.R., MacNee, W., Stone, V., Donaldson, K., 2001. Size-dependent proinflammatory effects of ultrafine polystyrene particles: a role for surface area and oxidative stress in the enhanced activity of ultrafines. Toxicol. Appl. Pharmacol. 175, 191–199.

Carter, J.M., Driscoll, K.E., 2001. The role of inflammation, oxidative stress, and proliferation in silica-induced lung disease: a species comparison. J. Environ. Pathol. Toxicol. Oncol. 20 (Suppl. 1), 33–43.

Chen, M., von Mikecz, A., 2005. Formation of nucleoplasmic protein aggregates impairs nuclear function in response to SiO_2 nanoparticles. Exp. Cell Res. 305, 51–62.

Chen, Y., Chen, J., Dong, J., Jin, Y., 2004. Comparing study of the effect of nanosized silicon dioxide and microsized silicon dioxide on fibrogenesis in rats. Toxicol. Ind. Health 20, 21–27.

Dalal, N.S., Shi, X.L., Vallyathan, V., 1990. Role of free radicals in the mechanisms of hemolysis and lipid peroxidation by silica: comparative ESR and cytotoxicity studies. J. Toxicol. Environ. Health 29, 307–316.

Donaldson, K., Borm, P.J., 1998. The quartz hazard: a variable entity. Ann. Occup. Hyg. 42, 287–294.

Donaldson, K., Tran, C.L., 2002. Inflammation caused by particles and fibers. Inhal. Toxicol. 14, 5–27.

Draper, H.H., Squires, E.J., Mahmoodi, H., Wu, J., Agarwal, S., Hadley, M., 1993. A comparative evaluation of thiobarbituric acid methods for the determination of malondialdehyde in biological materials. Free Radical Biol. Med. 15, 353–363.

Fenoglio, I., Prandi, L., Tomatis, M., Fubini, B., 2001. Free radical generation in the toxicity of inhaled mineral particles: the role of iron speciation at the surface of asbestos and silica. Redox. Rep. 6, 235–241.

Foncea, R., Carvajal, C., Almarza, C., Leighton, F., 2000. Endothelial cell oxidative stress and signal transduction. Biol. Res. 33, 89–96.

Fubini, B., Hubbard, A., 2003. Reactive oxygen species (ROS) and reactive nitrogen species (RNS) generation by silica in inflammation and fibrosis. Free Radical Biol. Med. 34, 1507–1516.

Gemeinhart, R.A., Luo, D., Saltzman, W.M., 2005. Cellular fate of a modular DNA delivery system mediated by silica nanoparticles. Biotechnol. Prog. 21, 532–537.

Hirsch, L.R., Stafford, R.J., Bankson, J.A., Sershen, S.R., Rivera, B., Price, R.E., Hazle, J.D., Halas, N.J., West, J.L., 2003. Nanoshell-mediated near-infrared thermal therapy of tumors under magnetic resonance guidance. Proc. Natl. Acad. Sci. U. S. A. 100, 13549–13554.

Huang, M., Khor, E., Lim, L.Y., 2004. Uptake and cytotoxicity of chitosan molecules and nanoparticles: effects of molecular weight and degree of deacetylation. Pharm. Res. 21, 344–353.

IARC, 1997. IARC Working Group on the Evaluation of Carcinogenic Risks to Humans: silica, some silicates, coal dust and para-aramid fibrils. Lyon, 15–22 October 1996. IARC Monogr. Eval. Carcinog. Risks Hum. 68, 1–475.

Kharasch, E.D., Schroeder, J.L., Bammler, T., Beyer, R., Srinouanprachanh, S., 2006. Gene expression profiling of nephrotoxicity from the sevoflurane degradation product fluoromethyl-2,2-difluoro-1-(trifluoromethyl)vinyl ether ("compound a") in rats. Toxicol. Sci. 90, 419–431.

Kipen, H.M., Laskin, D.L., 2005. Smaller is not always better: nanotechnology yields nanotoxicology. Am. J. Physiol.: Lung Cell Mol. Physiol. 289, L696–L697.

Lenz, A.G., Krombach, F., Maier, K.L., 1992. Oxidative stress in vivo and in vitro: modulation by quartz dust and hyperbaric atmosphere. Free Radical Biol. Med. 12, 1–10.

Nel, A., Xia, T., Madler, L., Li, N., 2006. Toxic potential of materials at the nanolevel. Science 311, 622–627.

Oberdörster, G., 2000. Toxicology of ultrafine particles: in vivo studies. Trans. R Soc. Lond. A 358, 2719–2740.

Oberdorster, G., Oberdorster, E., Oberdorster, J., 2005. Nanotoxicology: an emerging discipline evolving from studies of ultrafine particles. Environ. Health Perspect. 113, 823–839.

Peters, K., Unger, R.E., Kirkpatrick, C.J., Gatti, A.M., Monari, E., 2004. Effects of nano-scaled particles on endothelial cell function in vitro: Studies on viability, proliferation and inflammation. J. Mater. Sci., Mater. Med. 15, 321–325.

Porter, D.W., Millecchia, L.L., Willard, P., Robinson, V.A., Ramsey, D., McLaurin, J., Khan, A., Brumbaugh, K., Beighley, C.M., Teass, A., Castranova, V., 2006. Nitric oxide and reactive oxygen species production causes progressive damage in rats after cessation of silica inhalation. Toxicol. Sci. 90, 188–197.

Qhobosheane, M., Santra, S., Zhang, P., Tan, W., 2001. Biochemically functionalized silica nanoparticles. Analyst 126, 1274–1278.

Rimal, B., Greenberg, A.K., Rom, W.N., 2005. Basic pathogenetic mechanisms in silicosis: current understanding. Curr. Opin. Pulm. Med. 11, 169–173.

Santra, S., Zhang, P., Wang, K., Tapec, R., Tan, W., 2001. Conjugation of biomolecules with luminophore-doped silica nanoparticles for photostable biomarkers. Anal. Chem. 73, 4988–4993.

ayes, C.M., Liang, F., Hudson, J.L., Mendez, J., Guo, W., Beach, J.M., Moore, V.C., Doyle, C., West, D., Billups, J.L., Ausman, W.E., Colvin, K.D., 2006. Functionalization density dependence of single-walled carbon nanotubes cytotoxicity in vitro. Toxicol. Lett. 161, 135–142.

Shi, X., Castranova, V., Halliwell, B., Vallyathan, V., 1998. Reactive oxygen species and silica-induced carcinogenesis. J. Toxicol. Environ. Health, B Crit. Rev. 1, 181–197.

Skehan, P., Storeng, R., Scudiero, D., Monks, A., McMahon, J., Vistica, D., Warren, J.T., Bokesch, H., Kenney, S., Boyd, M.R., 1990. New colorimetric cytotoxicity assay for anticancer-drug screening. J. Natl. Cancer Inst. 82, 1107–1112.

Stix, G., 2001. Little big science. Nanotechnology. Sci. Am. 285, 32–37.

Venkatesan, N., Yoshimitsu, J., Ito, Y., Shibata, N., Takada, K., 2005. Liquid filled nanoparticles as a drug delivery tool for protein therapeutics. Biomaterials 26, 7154–7163.

Wacker, W.E.C., Ulmer, D.D., Vallee, B.L., 1956. Metalloenzymes and myocardial infarction: II. Malic and lactic dehydrogenase activities and zinc concentrations in serum. N. Engl. J. Med. 255, 450–456.

Wang, H., Joseph, J.A., 1999. Quantifying cellular oxidative stress by dichlorofluorescein assay using microplate reader. Free Radical Biol. Med. 27, 612–616.

Warheit, D.B., Reed, K., Webb, K., Sayes, C.M., Colvin, V.L., 2005. Pulmonary

toxicity screening studies with nano vs. fine-sized quartz and TiO2 particles in rats. Toxicologist 84 (S-1), A1043.

Winters, R.A., Zukowski, J., Ercal, N., Matthews, R.H., Spitz, D.R., 1995. Analysis of glutathione, glutathione disulfide, cysteine, homocysteine, and other biological thiols by high-performance liquid chromatography following derivatization by n-(1-pyrenyl)maleimide. Anal. Biochem. 227, 14–21.

Xue, Z.G., Zhu, S.H., Pan, Q., Liang, D.S., Li, Y.M., Liu, X.H., Xia, K., Xia, J.H., 2006. Biotoxicology and biodynamics of silica nanoparticle. Zhong Nan Da Xue Xue Bao Yi Xue Ban 31, 6–8.

Zhang, F.F., Wan, Q., Li, C.X., Wang, X.L., Zhu, Z.Q., Xian, Y.Z., Jin, L.T., Yamamoto, K., 2004. Simultaneous assay of glucose, lactate, L-glutamate and hypoxanthine levels in a rat striatum using enzyme electrodes based on neutral red-doped silica nanoparticles. Anal. Bioanal. Chem. 380, 637–642.